

## THE X-RAY SYSTEM R AQUARI: A TWO-SIDED JET AND CENTRAL SOURCE

E. KELLOGG,<sup>1</sup> J. A. PEDELTY,<sup>2</sup> AND R. G. LYON<sup>3</sup>

Received 2001 July 18; accepted 2001 November 8; published 2001 December 7

### ABSTRACT

We report *Chandra* ACIS-S3 X-ray imaging and spectroscopy of the R Aquarii binary system that show a spatially resolved two-sided jet and an unresolved central source. This is the first published report of such an X-ray jet seen in an evolved  $\sim 2\text{--}3 M_{\odot}$  stellar system. At  $E < 1$  keV, the X-ray jet extends to both the northeast (NE) and southwest (SW) relative to the central binary system. At  $1 < E < 7.1$  keV, R Aqr is a pointlike source centered on the star system. While both 3.5 cm radio continuum emission and X-ray emission appear coincident in projection and have maximum intensities at  $\sim 7''.5$  NE of the central binary system, the next strongest X-ray component is located  $\sim 30''$  SW of the central binary system and has no radio continuum counterpart. The X-ray jets are likely shock-heated in the recent past and are not in thermal equilibrium. The strongest SW X-ray jet component may have been shocked recently since there is no relic radio emission as expected from an older shock. At the position of the central binary, we detect X-ray emission below 1.6 keV consistent with blackbody emission at  $T \sim 2 \times 10^6$  K. There is also a prominent 6.4 keV feature, a possible fluorescence or collisionally excited Fe K $\alpha$  line from an accretion disk or from the wind of the giant star. For this excitation to occur, there must be an unseen hard source of X-rays or particles in the immediate vicinity of the hot star. Such a source would be hidden from view by the surrounding edge-on accretion disk.

*Subject headings:* binaries: symbiotic — circumstellar matter — radio continuum: stars — stars: individual (R Aquarii) — stars: winds, outflows — white dwarfs — X-rays: general

### 1. INTRODUCTION

R Aqr is a symbiotic stellar system: a mass-losing  $\sim 1\text{--}2 M_{\odot}$  Mira-like long-period variable (LPV) with a 387 day period and a  $\sim 1 M_{\odot}$  hot companion with many of its features explained by an accretion disk model. The companion is believed to give rise to the nonrelativistic jet seen at UV, optical, and radio wavelengths. Since no UV continuum is observed, the accretion disk is believed to be edge-on (Kafatos, Michalitsianos, & Hollis 1986). The binary system orbit has been characterized as highly inclined to the line of sight ( $i \sim 70^\circ$ ) with large eccentricity ( $e \sim 0.8$ ), a semimajor axis of  $\sim 2.6 \times 10^{14}$  cm, an orbital period of  $\sim 44$  yr, and at a distance of 200 pc (see Hollis, Pedelty, & Lyon 1997b, and references therein). Hence, the northeast (NE)–southwest (SW) oriented jet is probably refueled episodically with increased activity at periastron since the hot companion passes through the LPV’s outer envelope. It is further posited that the binary system was at apastron circa 1996 (Hollis, Pedelty, & Kafatos 1997a), so neither star should influence the other for many years near this epoch.

From the early 1980s to the present epoch, the dominant NE radio jet has undergone NE motion outward from the central H II region and counterclockwise rotation, i.e., precession about the central H II region (Hollis et al. 1997b). UV, optical, and radio observations of the NE jet are described as resulting from shock excitation (e.g., Hollis et al. 1991; Hollis, Dorband, & Yusef-Zadeh 1992; Hollis et al. 1997b) as the jet motion impacts the considerable circumstellar material from LPV mass loss. For example, the thermal bremsstrahlung radiation seen in the radio regime is suggested as a relic of a passing shock front. Shock modeling of the R Aqr NE radio and UV jets suggests that temperatures should be on the order of that re-

quired for X-ray emission (Hollis et al. 1997b). The R Aqr system was first reported as an unresolved *Einstein* X-ray source by Jura & Helfand (1984). It was later observed with *EXOSAT* (Viotti et al. 1987) and *ROSAT* (Hünsch et al. 1998), so we planned a *Chandra* observation to determine the spatial and spectral structure and nature of the R Aqr X-ray emission. Preliminary results were reported at HEAD 2000 (Kellogg et al. 2000).

### 2. OBSERVATIONS AND RESULTS

#### 2.1. *Chandra* Imaging and Spectra

*Chandra* observed R Aqr for 24.5 ks on 2000 September 10 (JD 2,451,797.7 start time) with the Advanced CCD Imaging Spectrometer (ACIS)-S3 back-illuminated chip, which records photon energy for imaging and spectroscopy. The ACIS-S3 pixel size is  $0''.492$  (*Chandra* X-Ray Center 2000, hereafter CXC). The *Chandra* ACIS-S3 on-axis point-spread function in the 0.3–1.0 keV range has 50% and 80% encircled energy radii of  $\sim 0''.418$  and  $\sim 0''.685$ , respectively (CXC). A spatial image was constructed from the standard pipeline processed data. X-ray events were extracted from a  $0.38$  arcmin<sup>2</sup> region (5668 pixels) encompassing the jets and central source, yielding 1540 total counts in 22,717 s, or  $0.068$  counts s<sup>−1</sup>.

Figure 1 is a contour image of smoothed *Chandra* data showing a resolved NE jet, an unresolved central source, and a resolved multicomponent SW jet. The Figure 1 image was shifted in position by  $\sim 0''.4$  in right ascension and  $\sim 0''.6$  in declination to align the peaks of the unresolved source in the X-ray and radio images (see § 2.2 below). The *Chandra* absolute position uncertainty has a  $1 \sigma$  error circle radius of  $0''.6$  (CXC), while the radio positions are accurate to  $0''.1$ , one-tenth of the restoring beam size.

Spectra of the NE jet, the central source, and the SW jet were extracted using CIAO *Chandra* analysis routines and XSPEC (Arnaud 1996). Figure 2 shows the extraction regions, spectra, and fits. In spite of small numbers of counts, the spectra

<sup>1</sup> Harvard-Smithsonian Center for Astrophysics, 60 Garden Street, MS 27, Cambridge, MA 02138.

<sup>2</sup> Biospheric Sciences Branch, Code 923, NASA Goddard Space Flight Center, Greenbelt, MD 20771.

<sup>3</sup> Instrument Technology Center, Code 550, NASA Goddard Space Flight Center, Greenbelt, MD 20771.

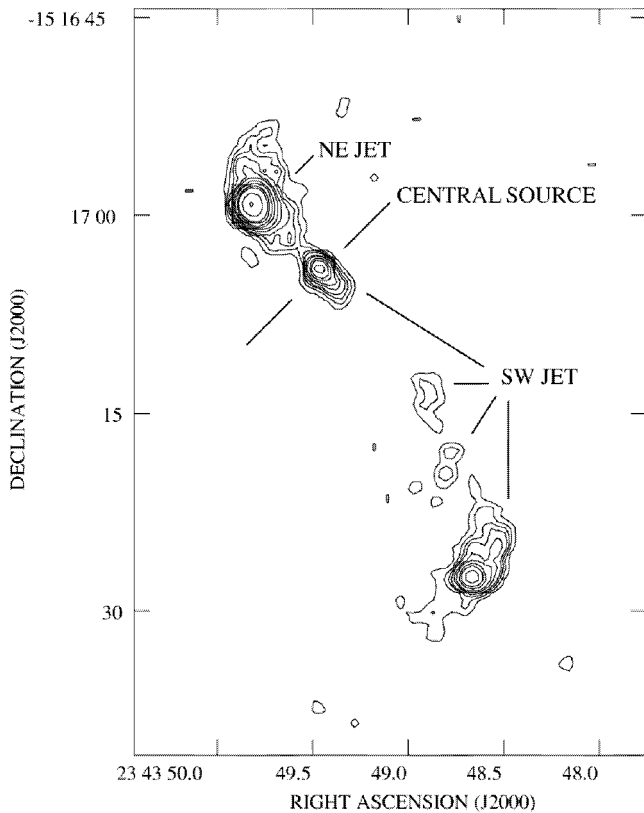


FIG. 1.—Contour map of the R Aqr 0.1–10 keV X-ray image showing the NE jet, central source, and SW jet. The original ACIS image has been convolved with a 1" FWHM circular Gaussian to facilitate smooth contours. The peak photon count in this image is 194.4 counts, and the contour levels are 1.4, 2.8, 4.2, 5.6, 8.4, 11.2, 16.8, 22.4, 33.6, 44.8, 89.6, and 179.2 counts. At  $E > 1$  keV, the jets are not visible; the dominant emission comes from a point-like source at the star system.

required complex models for reasonable fits. A nonequilibrium collisional excitation model was used for the jets (Borkowski, Lyerly, & Reynolds 2001) with Anders & Grevesse (1989, hereafter AG) initial abundances, with varying abundances for the SW jet (see Table 1). Data were binned into 15 counts channel<sup>-1</sup> for the NE and SW jets and 114 eV channels for the central region. We fitted the interstellar column density (the XSPEC WABS model). Results were consistent with radio observations of  $1.84 \times 10^{20}$  cm<sup>-2</sup> (Stark et al. 1992). The NE jet shows two peaks, at  $\sim 400$  and  $550$  eV, and has few counts above 1 keV. The Raymond & Smith (1977) model gave a temperature in the  $2 \times 10^6$  K range with less than 1% confidence. It gave only a peak at the O VII line complex,  $\sim 570$  eV, increasing only to 6% confidence with variable abundances (the calculated N peak in that case was too broad to fit the data well, due to a complex of lines present in the model). Therefore, we used the NEI collisional excitation XSPEC model (Borkowski et al. 2001). This gave an acceptable fit, including a second peak at  $\sim 430$  eV. The SW jet spectrum has only one peak at  $\sim 550$  eV. A Raymond-Smith fit gave a calculated peak at a higher energy than observed and only 7% confidence, not improved by varying the abundances from the AG values. The XSPEC MEKAL models gave similar results. A good fit was obtained using the NEI model only with relative O abundances  $\geq 20$ . At relative O abundances of less than 20, the calculated O peak was at a higher energy than the data peak. More com-

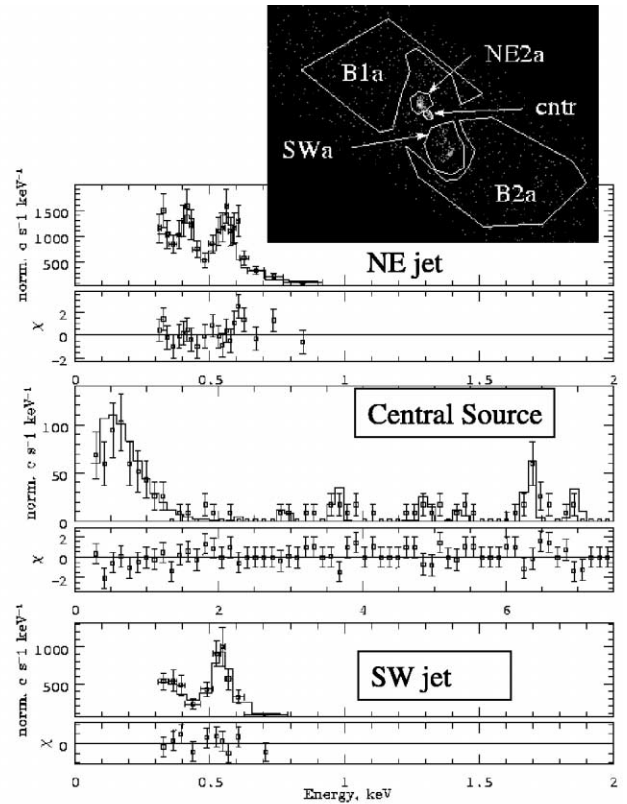


FIG. 2.—R Aqr X-ray spectrum extraction regions and spectral fits. The upper panel shows the raw image with source and background spectral extraction regions; NE2a and B1a for the NE jet, cntr and B2a for the central source, and SWa and B2a for the SW jet. The plots show the spectra of the NE jet, central source, and SW jet with best-fit models. The NE jet data, binned to 15 counts channel<sup>-1</sup>, has peaks from expected O VII emission at 0.574 keV and N VI at 0.43 keV. The histogram fit is a nonequilibrium ionization model with interstellar absorption. The central source data, binned in 114 eV width channels, is modeled by a blackbody, a Fe K $\alpha$  line at  $\sim 6.4$  keV, K $\beta$  at  $\sim 7.0$  keV, and other discrete but weak lines at K energies of Cr, V, Ca, Ar, and S. The Fe line suggests a hidden hard source associated with an accretion disk. The SW X-ray jet data, binned to 15 counts per channel, has the expected O VII peak at 0.574 keV. The fit is to a nonequilibrium ionization model with high O abundance (e.g., see Table 4 of Hollis et al. 1991).

plex collisional excitation models having more free parameters did not improve the fit.

In Figure 2, we also show a fit to a blackbody for the central source at low energies, and nine Gaussians at expected K line energies of Fe and the lighter even-Z elements, down to 1.6 keV, where the blackbody model dominates. We quote the blackbody fit parameters in Table 1, although we could not reject equilibrium optically thin hot gas models at the 50% confidence level. The hard central source shows a feature containing 16 counts with a flux of  $4.9 \pm 1.7 \times 10^{-14}$  ergs cm<sup>-2</sup> s<sup>-1</sup> at  $6.41 \pm 0.04$  keV. This could be Fe I (i.e., K $\alpha$ ), or up to Fe IV, based on the calculations tabulated in Kaastra & Mewe (1993), or up to Fe X based on the measurements of Decaux et al. (1997). There are also suggestions of emission from Fe K $\beta$  at 7.1 keV, 3 counts, and emission from K $\alpha$  lines of Ca, V, and Cr: 7 counts at 3.7 keV, 6 counts at 5.0 keV, and 4 counts at 5.4 keV, respectively. The expected number of background counts in each channel is a few times  $10^{-2}$ ; there are essentially no background counts in this energy range. This was checked by displacing the central source region about 1"; it contained no counts. Our data are very likely real X-ray emission events from the central source.

TABLE 1  
SPECTRAL FIT PARAMETERS

JETS: NONEQUILIBRIUM IONIZATION MODEL WITH INTERSTELLAR ABSORPTION		
Quantity	NE Jet	SW Jet
Counts in spectrum, $E > 0.3$ keV	396	196
C abundance (fraction of AG)	1.0 (fixed)	$\leq 0.5$
N abundance (fraction of AG)	1.0 (fixed)	0. (fixed)
O abundance (fraction of AG)	1.0 (fixed)	20 (fixed)
$n_{\text{H}}$ ( $10^{20} \text{ cm}^{-2}$ )	$\leq 5.4 \pm 1.5$	$\leq 10$
$kT$ (keV)	$1.66 \pm 0.99$	$0.20 \pm 0.06$
$T$ (K)	$19.3 \pm 11.5$	$2.3 \pm 0.7$
$\tau$ , ionization timescale ( $\text{s cm}^{-3}$ )	$4.3 \pm 0.3 \times 10^8$	$1.9 \pm 0.5 \times 10^8$
Normalization ( $10^{-5} \text{ photons cm}^{-2} \text{ s}^{-1} \text{ keV}^{-1}$ )	$4.0 \pm 1.0 \times 10^{-5}$	$1.5(0.8-7.1) \times 10^{-4}$
Observed flux ( $10^{-14} \text{ ergs cm}^{-2} \text{ s}^{-1}$ )	$7.1 \pm 1.8$	$2.6(1.4-12.3)$
Source flux ( $n_{\text{H}} = 0, 10^{-14} \text{ ergs cm}^{-2} \text{ s}^{-1}$ )	$18.9 \pm 4.7$	$3.1(1.7-14.7)$
Reduced $\chi^2$	1.04	1.19
Confidence (%) <sup>a</sup>	41	31

CENTER SOFT SOURCE: BLACKBODY WITH INTERSTELLAR ABSORPTION	
Quantity	Center Source
Counts in spectrum, $E > 0.3$ keV	108
$n_{\text{H}}$ ( $10^{20} \text{ cm}^{-2}$ )	$\leq 6.2$
$kT$ (keV)	$0.18 \pm 0.02$
$T$ ( $10^6$ K)	$2.09 \pm 0.23$
Normalization ( $10^{-5} \text{ photons cm}^{-2} \text{ s}^{-1} \text{ keV}^{-1}$ )	$0.009 \pm 0.005$
Observed flux ( $10^{-14} \text{ ergs cm}^{-2} \text{ s}^{-1}$ , 0.3–2.0 keV)	$0.68 \pm 0.38$
Source flux ( $n_{\text{H}} = 0, 10^{-14} \text{ ergs cm}^{-2} \text{ s}^{-1}$ , 0.3–2.0 keV)	$0.68 \pm 0.38$
Reduced $\chi^2$	0.55
Confidence (%)	84

NOTE.—All errors are  $1 \sigma$ .

<sup>a</sup> XSPEC null hypothesis probability.

We observed a flux of  $1.0 \pm 0.2 \times 10^{-13} \text{ ergs cm}^{-2} \text{ s}^{-1}$  at  $E < 2$  keV from R Aqr. Hünsch et al. (1998) observed 5 times greater flux in that energy range during the *ROSAT* All Sky Survey, epoch 1990–1991. We also observed an additional  $1.0 \pm 0.25 \times 10^{-13} \text{ ergs cm}^{-2} \text{ s}^{-1}$  at  $E > 2$  keV, not visible to *ROSAT*. Viotti et al. (1987) inferred  $\sim 2 \times 10^{-11} \text{ ergs cm}^{-2} \text{ s}^{-1}$  by estimating the spectrum of the source. They also interpreted the *Einstein* report as an upper limit that corresponds to  $\sim 2.5 \times 10^{-13} \text{ ergs cm}^{-2} \text{ s}^{-1}$ . We conclude that R Aqr is several times fainter in our data than it was in the 1980s and early 1990s.

## 2.2. VLA Imagery

R Aqr was observed on 1999 November 1, 4, and 7 with the NRAO<sup>4</sup> Very Large Array in the B configuration. Two sets of receivers were combined to observe a 100 MHz band centered at a frequency of 8460.1 MHz ( $\sim 3.5$  cm wavelength). A total of  $\sim 2$  million visibilities were accumulated in  $\sim 8$  hr of on-source integration. AIPS software was used for standard calibration and imaging. The resulting uniformly weighted image is thermal noise limited ( $1 \sigma$  noise level of  $8 \mu\text{Jy}$ ) and has a restoring beam of  $1''.00 \times 0''.69$  with a major-axis position angle of  $-3^\circ 9$ . The NE radio jet is shown as contours in Figure 3 overlaid on a color image of the NE X-ray jet, and both jets are seen in projection to be spatially coincident.

## 3. DISCUSSION

The R Aqr symbiotic star system is strikingly different at  $E < 1$  keV than from 1–7 keV. At the lower energy, the jets dominate. Above 1 keV, R Aqr looks pointlike at the *Chandra* resolution, centered on the star system. The X-ray jets are another manifestation of directed flow seen in the radio, optical, and UV. This is solid evidence for cylindrical accretion geometry, i.e., a disk. Hollis & Koupelis (2000) developed a parcel ejection model for the R Aqr jet emitted along the rotation axis of the massive rotating star–accretion disk system that anchors a magnetic field. A natural extension of the model suggests that the X-ray emission from the jet could be the result of shock emission as the jet parcel plows into the ambient circumstellar medium. The preservation of a well-defined direction for the jets, with evidence for precession, argues against simple spherical accretion. In Figure 1, the strongest parcel in the SW jet seems to have contour compression on its SW edge as would result from SW directed motion. The NE jet component has contour compression on its eastern edge that may be due to counterclockwise motion about the central source reported previously for the NE radio jet (Hollis et al. 1997b). In Figure 3, the NE X-ray jet as seen in projection lies along the same trajectory as the NE radio jet, supporting a counterclockwise rotation scenario for the NE X-ray jet. The 430 eV peak in the NE jet and the need for the NEI model to fit the spectrum suggests that this feature was formed recently, with a product of age and ambient density of  $4.3 \times 10^8 \text{ s cm}^{-3}$ . If  $n \sim 1 \text{ cm}^{-3}$  as for the typical interstellar medium, the age is  $\sim 15$  yr. This is comparable to the observed timescale for changes in the radio emission, and in X-ray, as inferred from comparing our data with the earlier X-ray satellite observations.

<sup>4</sup> The National Radio Astronomy Observatory is operated by Associated Universities, Inc., under cooperative agreement with the National Science Foundation.

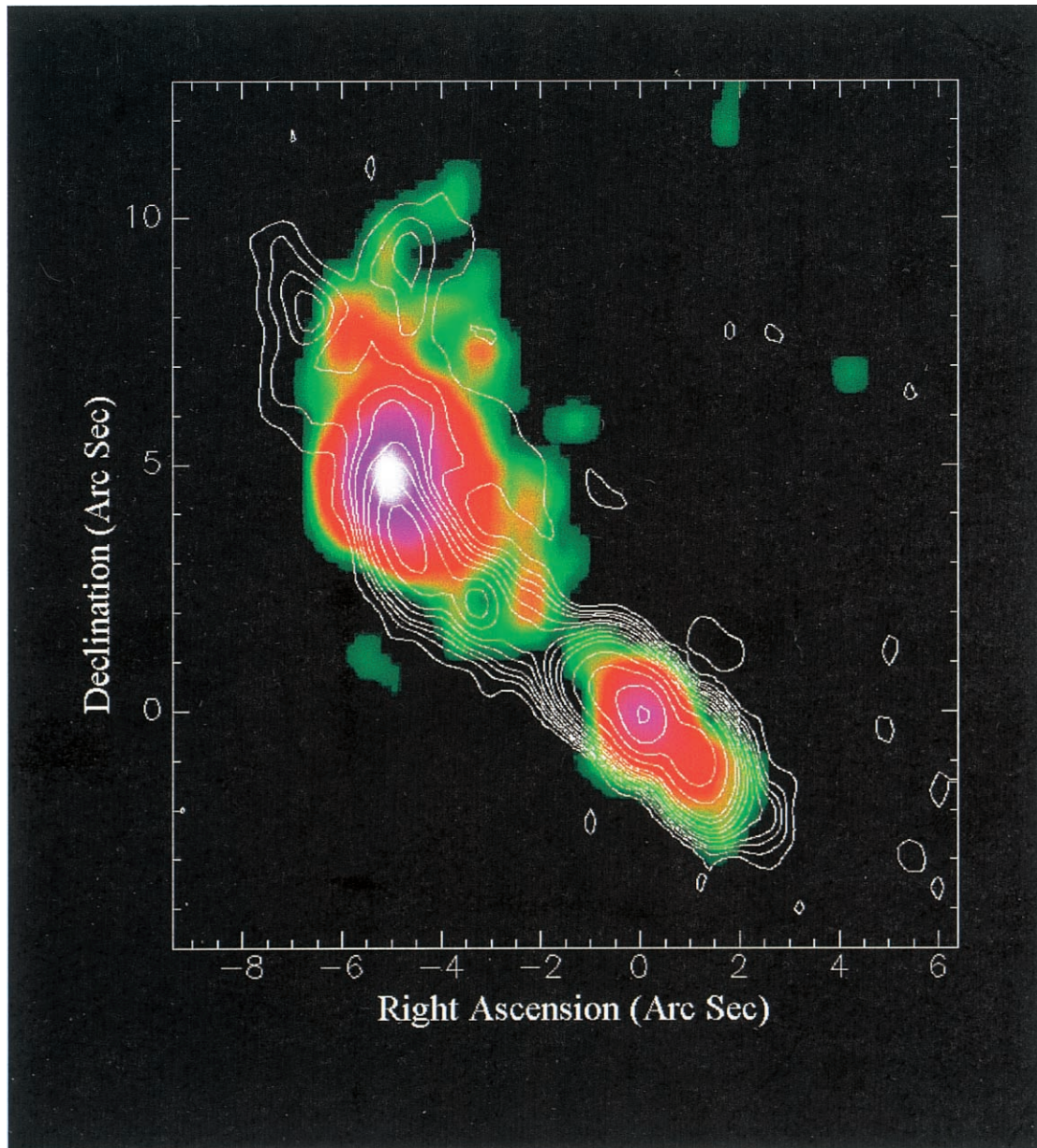


FIG. 3.—Color rendering of the *Chandra* ACIS image of the R Aqr NE jet and central H II region overlaid with a contour plot of the 3.5 cm radio continuum emission, observed 10 months earlier. The coordinate system is defined relative to the peaks of the X-ray and radio continuum emission (assumed coincident). The X-ray image has been convolved with a  $1''.00 \times 0''.69$  elliptical Gaussian that is the same size as the restoring beam of the radio image. The peak flux is  $10.94 \text{ mJy beam}^{-1}$ , and the contour levels are 0.02, 0.04, 0.06, 0.08, 0.12, 0.16, 0.24, 0.32, 0.48, 0.64, 1.28, 2.56, 5.12, and  $10.24 \text{ mJy beam}^{-1}$ .

For greater density, as might be expected near the R Aqr Mira, the age may be less. The SW X-ray jet is  $\sim 30''$  from the central source compared with  $\sim 7''.5$  for the NE jet, suggesting that it was ejected earlier. It has a different spectrum, with no N peak. We could only fit a model with a very high O abundance. Either there is a velocity shift in the O peak, or there is a different mix of the O VII lines at 0.569, 0.574, and 0.666 keV than our models can reproduce. The derived value of the ionization timescale is about half that of the NE jet, so given the expected variation in ISM density, the time since heating may be about the same. However, if the SW jet was shocked further in the past, we should expect to see relic radio emission as in the NE jet that is not detected. The shock temperatures from the two NEI fits to the jets seem disparate but differ only by  $\sim 1.5 \sigma$ , so the difference is not very significant. The central X-ray source has a counterpart in 3.5 cm radio continuum (cf.

Fig. 3). The radio emission is a thermal H II region at  $\sim 10^4 \text{ K}$ , while the central X-ray source low-energy spectrum in Figure 2 fits indicates a temperature of order  $10^6 \text{ K}$ . Perhaps the X-ray-emitting volume is interior to the H II region, associated with a high energy density region at the hot star/accretion disk. The neutral or lightly ionized Fe at 6.4 keV, without strong associated continuum, is evidence for relatively cooler material excited by an unseen source of hard photons or charged particles. Such emission could be reflecting from the surface of the edge-on accretion disk (e.g., Frank, King, & Raine 1992, p. 203) or directly exciting the relatively cool material at the boundary of a surrounding Stromgren surface.

#### 4. SUMMARY

We have imaged a two-sided X-ray jet and detected an unresolved central X-ray source in the R Aqr binary system with

*Chandra* ACIS-S3. Nonequilibrium collisional ionization models were applied to the jets. Both jets have ionization timescales of  $\sim 10^8$  s  $\text{cm}^{-3}$ , corresponding to ages of order 10 yr or less. A 6.4 keV feature in the central source must be a deexcitation line of relatively cool gas, evidence of an unseen hard source near the hot star, hidden from view owing to the surrounding edge-on accretion disk. Comparison of the NE X-ray jet and central X-ray source with 3.5 cm radio continuum VLA imagery at the same resolution suggests that the X-ray jet may be a high-temperature, low-density region associated with

cooler postshock UV- and radio-emitting regions. After more than 100 years of intense study, R Aqr is still revealing new and fascinating features.

We thank Eric Feigelson, Steve Drake, John Raymond, and Brad Wargelin for useful discussions and the referee for a thorough reading of the manuscript and suggestions for improvement. We acknowledge support from NASA grant GO0-1062A. E.-K. received support from NASA contract NAS8-39073. J. A. P. received support from NASA RTOP 344-02-03-01.

## REFERENCES

- Anders, E., & Grevesse, N. 1989, *Geochim. Cosmochim. Acta*, 53, 197 (AG)
- Arnaud, K. A. 1996, in *ASP Conf. Ser. 101, Astronomical Data Analysis Software and Systems V*, ed. G. H. Jacoby & J. Barnes (San Francisco: ASP), 17
- Borkowski, K. J., Lyerly, W. J., & Reynolds, S. P. 2001, *ApJ*, 548, 820
- Chandra* X-Ray Center. 2000, *The Chandra Proposers' Observatory Guide*, Version 3.0, TD403.00.003 (CXC)
- Decaux, V., Beiersdorfer, P., Kahn, S. M., & Jacobs, V. L. 1997, *ApJ*, 482, 1076
- Frank, J., King, A., & Raine, D. 1992, *Accretion Power in Astrophysics* (2d ed.; Cambridge: Cambridge Univ. Press)
- Hollis, J. M., Dorband, J. E., & Yusef-Zadeh, F. 1992, *ApJ*, 386, 293
- Hollis, J. M., & Koupelis, T. 2000, *ApJ*, 528, 418
- Hollis, J. M., Oliverson, R. J., Michalitsianos, A. G., Kafatos, M., & Wagner, R. M. 1991, *ApJ*, 377, 227
- Hollis, J. M., Pedelty, J. A., & Kafatos, M. 1997a, *ApJ*, 490, 302
- Hollis, J. M., Pedelty, J. A., & Lyon, R. G. 1997b, *ApJ*, 482, L85
- Hünsch, M., Schmitt, J. H., Schroeder, K., & Zickgraf, F. 1998, *A&A*, 330, 225
- Jura, M., & Helfand, D. J. 1984, *ApJ*, 287, 785
- Kaastra, J. S., & Mewe, R. 1993, *A&AS*, 97, 443
- Kafatos, M., Michalitsianos, A. G., & Hollis, J. M. 1986, *ApJS*, 62, 853
- Kellogg, E., Hollis, J. M., Pedelty, J. A., & Lyon, R. G. 2000, *AAS HEAD Meeting*, 32, 25.08
- Raymond, J. C., & Smith, B. W. 1977, *ApJS*, 35, 419
- Stark, A. A., Gammie, C. F., Wilson, R. W., Bally, J., Linke, R. A., Heiles, C., & Hurwitz, M. 1992, *ApJS*, 79, 77
- Viotti, R., Piro, L., Friedjung, M., & Cassatella, A. 1987, *ApJ*, 319, L7